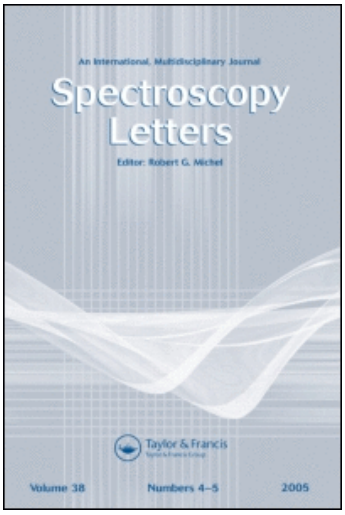

Spectroscopy Letters
Publication details, including instructions for authors and subscription information:
http://www.informaworld.com/smpp/title~content=t713597299

Analysis of Upconversion Fluorescence Dynamics in $NaYF_4$ Codoped with Er^{3+} and Yb^{3+}

W. Wang[a]; Mingmei Wu[b]; G. K. Liu[a]
[a] Chemistry Division, Argonne National Laboratory, Argonne, Illinois, USA [b] State Key Laboratory of Optoelectronic Materials and Technologies, School of Chemistry and Chemical Engineering, Sun Yat-Sen (Zhongshan) University, Guangzhou, People's Republic of China

To cite this Article Wang, W. , Wu, Mingmei and Liu, G. K.(2007) 'Analysis of Upconversion Fluorescence Dynamics in $NaYF_4$ Codoped with Er^{3+} and Yb^{3+}', Spectroscopy Letters, 40: 2, 259 — 269
To link to this Article: DOI: 10.1080/00387010701247399
URL: http://dx.doi.org/10.1080/00387010701247399

Spectroscopy Letters, 40: 259–269, 2007

ISSN 0038-7010 print/1532-2289 online
DOI: 10.1080/00387010701247399

Analysis of Upconversion Fluorescence Dynamics in $NaYF_4$ Codoped with Er^{3+} and Yb^{3+}

W. Wang
Chemistry Division, Argonne National Laboratory, Argonne, Illinois, USA

Mingmei Wu
State Key Laboratory of Optoelectronic Materials and Technologies, School of Chemistry and Chemical Engineering, Sun Yat-Sen (Zhongshan) University, Guangzhou, People's Republic of China

G. K. Liu
Chemistry Division, Argonne National Laboratory, Argonne, Illinois, USA

Abstract: The efficiency of upconversion fluorescence for Er^{3+} and Yb^{3+} codoped into $NaYF_4$ powder crystals is investigated. The dependence of Er^{3+} green (540 nm) and red (660 nm) upconversion fluorescence intensities on laser excitation intensity and the ratio of the green and red fluorescence intensities respectively under 355-nm and 936-nm excitations have been measured and analyzed in terms of radiative and nonradiative relaxation mechanisms. It is shown that the intensity of both the green and red upconversion fluorescence bands is affected at high pumping intensities by a low-lying state acting as a bottleneck, with the red fluorescence less affected than the green. In addition to two-photon, two-step excitation and energy transfer processes, nonlinear optical coupling mechanisms of avalanche

Received 17 June 2006, Accepted 11 July 2006

The authors were invited to contribute this paper to a special issue of the journal entitled "Spectroscopy of Lanthanide Materials." This special issue was organized by Professor Peter Tanner, City University of Hong Kong, Kowloon.

Address correspondence to G. K. Liu, Chemistry Division, Argonne National Laboratory, Argonne, IL 60439, USA. E-mail: gkliu@anl.gov

processes appear responsible for reducing the bottleneck saturation of the red upconversion fluorescence.

Keywords: Excited state dynamics, green phosphor, unconversion fluorescence

INTRODUCTION

Excitation of a high-lying electronic state of lanthanide ions in inorganic solids that emits photons of energy higher than the excitation source, well-known as energy upconversion, is generally understood in the framework of quantum theory.[1] Driven by potential applications in new phosphors, laser materials, and enhanced detection of IR light, the upconversion phenomena in various materials have been extensively investigated. Because of their unique electronic energy level structures and solid-state optical properties, the lanthanide ions of Er^{3+} and Tm^{3+} have much higher quantum efficiency of unconversion fluorescence emission respectively in the green and blue region than any other ions of the series. In order to enhance upconversion efficiency, which is largely limited by the low $4f-4f$ transition probability and by self-quenching in the emitting states due to ion–ion interactions, codoping of Yb^{3+} with Er^{3+} or Tm^{3+} results in a significant increase in the efficiency of upconversion fluorescence.

A variety of Yb, Er and Yb, Tm codoped upconversion phosphors were synthesized and characterized.[2–8] Page et al.[3] have analyzed the upconversion efficiency as a function of excitation power. The previously studied phosphors are either single crystals or powders of different compositions codoped with Er^{3+} and Yb^{3+} and with Tm^{3+} and Yb^{3+}. The Er^{3+} green phosphors are the most efficient, yielding efficiency values as high as 4%, whereas the red and blue upconversion fluorescence have an efficiency of 1–2%. In the modeling, quasi-CW (continuous wave) modeling of the intensity-dependent upconversion efficiency was attempted; input data included level lifetimes, transition cross sections, and cross-relaxation rate coefficients. The saturation of the upconversion fluorescence with Yb and Er concentration in fluoride media was explained by the pumping of Er^{3+} ions into a bottleneck (long-lived state), that is, the $^4I_{13/2}$ metastable level, making them unavailable for further excitation transfer.

Hexagonal sodium yttrium fluoride ($NaYF_4$) has been identified as the most efficient host material for green (Er^{3+}) and blue (Tm^{3+}) upconversion phosphors that emits visible photons upon IR excitation.[2–4] Liang et al. have recent-reported efficient green upconversion of Er^{3+} in $NaYF_4$:Er/Yb of hexagonal structure synthesized using a hydrothermal method.[4] It was shown that the intensity ratio of green versus red fluorescence decreases as the concentration of Er^{3+} and Yb^{3+} increases. The optimal concentration of Er^{3+} less than 2% and Yb^{3+} less than 20%. In the lattice of $NaYF_4$, Y^{3+} can be replaced in any ratio by lanthanide ions such as Yb^{3+} and Er^{3+} or by

Yb^{3+} and Tm^{3+} for green or blue upconversion phosphors, respectively. Kano et al.[9] measured the green upconversion efficiency for Yb, Er codoped samples as a function of composition and firing temperature. The optimum conditions were found to be 30–40% Yb, 3–4% Er, and 630°C. Menyuk et al.[10] investigated a sample with 18% Yb and 2% Er prepared at 1000°C.

Although many theoretical analyses and phenomenal modeling of upconversion fluorescence have been performed, a consistent and systematic understanding of upconversion dynamics has not been satisfactorily established, for instance, one cannot clearly explain why the upconversion efficiency in hexagonal sodium yttrium fluoride is superior to that of other hosts. The mechanisms that determine the intensity ratio of the green (540 nm) fluorescence to the red (660 nm) fluorescence are not clearly understood. Furthermore, these upconversion fluorescences exhibit anomalous excitation-power dependences.[11,12] In the current work, we investigate the upconversion fluorescence dynamics of powder samples of $NaYF_4$ codoped with Yb^{3+} and Er^{3+} ions. The relative intensities of green and red fluorescence bands of Er^{3+} induced by a tunable CW Ti:sapphire laser were measured and analyzed based on the rate equations of various relaxation channels.

MATERIALS AND METHODS

The powder samples of $NaYF_4$:Yb_x/Er_y were prepared hydrothermally as described previously.[4] Of the three samples with different Er^{3+} and Yb^{3+} concentration respectively at $Yb_{0.2}/Er_{0.01}$, $Yb_{0.2}/Er_{0.015}$, and $Yb_{0.2}/Er_{0.02}$, the sample of $NaYF_4$:$Yb_{0.2}/Er_{0.015}$ exhibits the highest efficiency of upconversion fluorescence. The experimental results presented in this paper are from that sample.

To obtain the upconversion fluorescence spectrum of Er^{3+} ion in $NaYF_4$, a tunable continuous wave Ti:sapphire laser was used to pump the samples, which were mounted in a cryostat. The regular downconversion fluorescence spectrum of Er^{3+} was recorded using a pulsed (5 ns) Nd:YAG laser whose output was frequency tripled to 355 nm. The corresponding excitation, relaxation, and fluorescence transitions of Er^{3+} are shown in Figure 1. The fluorescence emission was dispersed by a Spex 1704 monochromator at a spectral resolution of around 0.008 nm and detected with a cooled RCA C31034 photomultiplier (USA). The signals were recorded using a lock-in amplifier for CW-laser pumping and a gated boxcar for pulsed-laser pumping. The fluorescence decay measurements were performed using a digital-storage oscilloscope (Tektronix TDS 680C) with 355-nm laser excitation. All the measurements were performed between 77 K and room temperature. The emission spectra have been calibrated based on the various grating and photomultiplier efficiencies at different wavelengths. A series of neutral-density filters were used to reduce the laser power in the measurements of power dependence of upconversion fluorescence intensity.

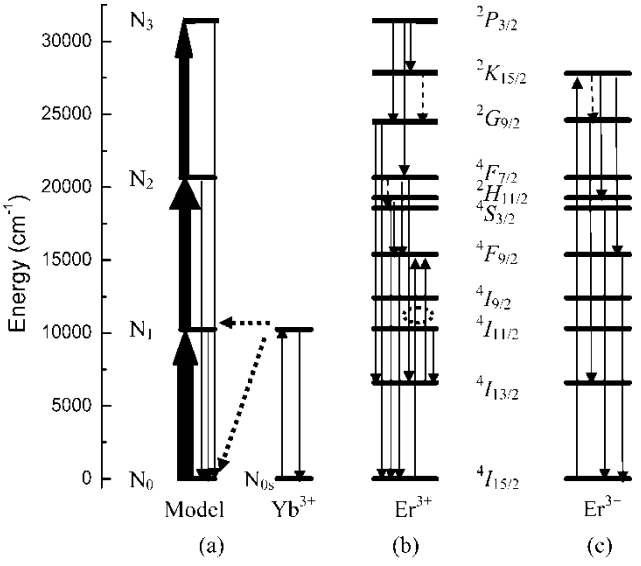

Figure 1. (a) General upconversion model; (b) transitions for the red and green emission of Er^{3+} under upconversion excitation; (c) red and green emission of Er^{3+} with Nd:YAG 355-nm pumping. Transitions circled with a dotted line in (b) are additional upconversion processes that contribute to the population of $^4F_{9/2}$. Direct transitions are indicated with solid lines. Dotted lines indicate energy transfer paths. The vertical dashed line shows important nonradiative relaxation processes.

RESULTS AND DISCUSSION

Upconversion and regular downconversion fluorescence bands of Er^{3+} from a powder sample of $NaYF_4:Yb_{0.2}/Er_{0.015}$ were recorded at both room temperature and 78 K. Figure 2 shows the upconversion spectrum of the sample at 78 K. A very intense green fluorescence band centered at 18,315 cm^{-1} was observed corresponding with $^4S_{3/2} \rightarrow {}^4I_{15/2}$ transitions. A red fluorescence band centered at 15,151 cm^{-1} is due to $^4F_{9/2} \rightarrow {}^4I_{15/2}$ transitions. In addition to the green and red fluorescence bands induced by upconversion requiring up to twice the energy of photons of the pumping laser, a weak upconversion fluorescence band with energy of 17,938 cm^{-1} corresponding with $^2G_{9/2} \rightarrow {}^4I_{13/2}$ transitions and a purple luminescence band centered approximately at 24,300 cm^{-1} of $^2G_{9/2} \rightarrow {}^4I_{15/2}$ transitions were also observed, which requires more than twice the photon energy of the pumping laser.

The ratio of the peak areas for the green band versus the red band is 4.68, which is significantly different from the value of 1.12 found for the ratio of those two emission bands when induced by 355-nm laser excitation. Figure 3 shows the emission spectrum of the sample at 78 K, pumped by

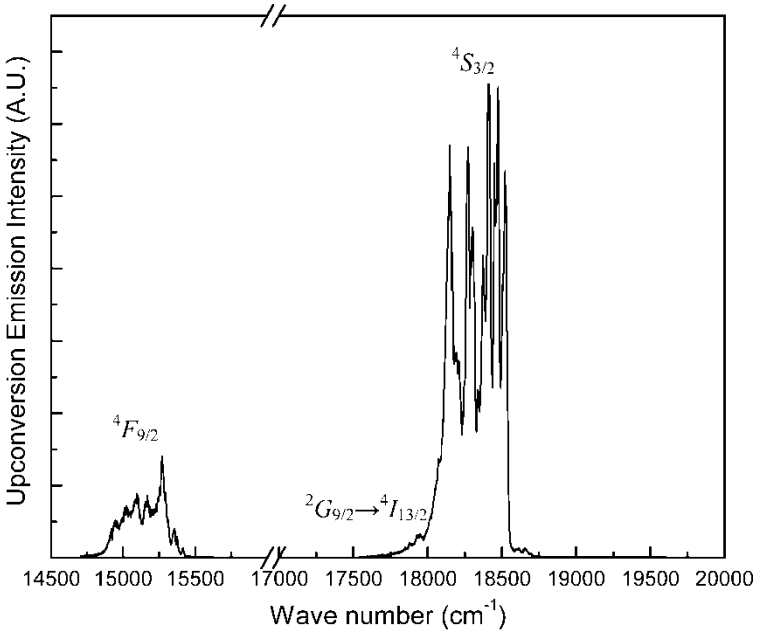

Figure 2. Upconversion spectrum of $NaYF_4$:$Yb_{0.2}/Er_{0.015}$ at 78 K, with 935.6-nm Ti-sapphire laser pumping.

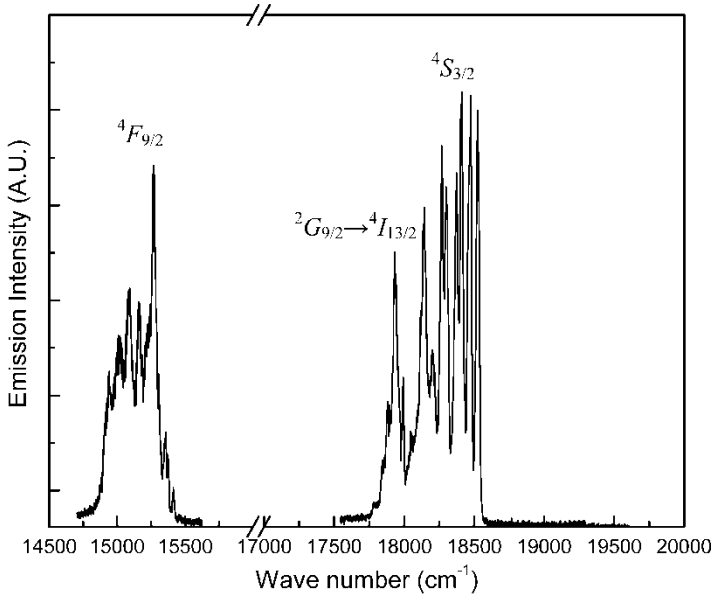

Figure 3. Emission spectrum of $NaYF_4$:$Yb_{0.2}/Er_{0.015}$, induced by 355-nm pulsed laser pumping the sample at 78 K.

the Nd:YAG pulsed laser at 355 nm. In this case, Er^{3+} is excited directly to $^2K_{15/2}$, then depleted to the ground state and lower-lying excited states, such as $^4F_{9/2}$ and $^4S_{3/2}$, through complex multiphonon process and radiative transitions between energy levels as shown in Figure 1c.

With 355-nm excitation, we also observe the fluorescence of transitions between $^2G_{9/2}$ and $^4I_{13/2}$ at 17,938 cm^{-1} close to the green band. The appearance of eight well-separated sharp peaks of the green band for the $^4S_{3/2} \rightarrow {}^4I_{15/2}$ transition is from the $J + (1/2)$ crystal-field splitting of the ground multiplet $^4I_{15/2}$. Considering only two phases reported in the literature for the $NaYF_4$ compound,[5–8] the observed splitting of the ground state into all its $J + (1/2) = 8$ crystal-field levels is consistent with a hexagonal (or lower symmetry) crystalline structure in the sample we studied. In the red fluorescence band at 78 K as shown in Figure 2 and Figure 3, there are more than eight lines, which indicates, in addition to the eight ground-state crystal-field levels, there is a hot band from at least one of the upper levels of the excited state $^4F_{9/2}$ along with the transitions from the lowest level of the excited state.

The excitation laser-power dependence of the upconversion fluorescence was measured at room temperature for the green and red fluorescence bands. As shown in Figure 4, one can see, with increase of laser intensity, the upconversion fluorescence intensity exhibits a quadratic dependence on laser intensity when the laser intensity is less than 1.4 W/cm^2. At higher laser intensities, the slope of the log plot for fluorescence intensity versus laser intensity

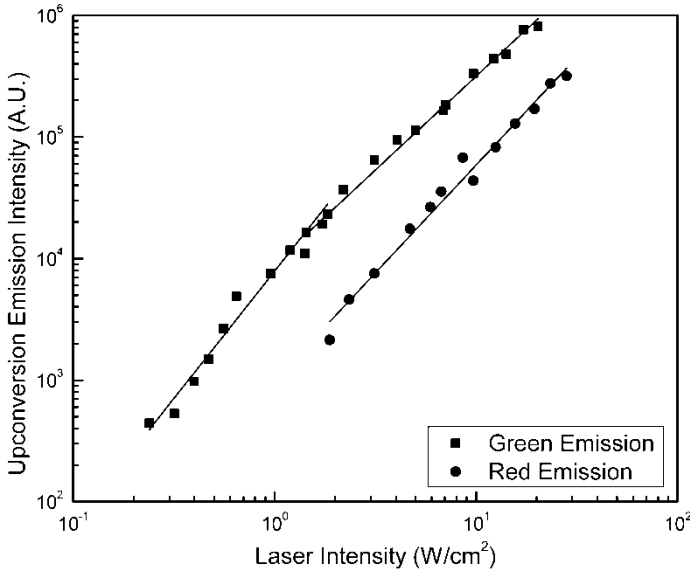

Figure 4. Log-log plots of the green and red upconversion emission intensities as a function of Ti-sapphire laser intensity on the sample.

reduces from 2 to 1.55 for the green band. Over the same laser intensity range, the slope for the red fluorescence is 1.78, apparently higher than that of the green band. At high laser power, the upconversion luminescence appears yellower than that at low-power pumping. This difference in laser intensity dependence suggests that the upconversion channels to populate $^4S_{3/2}$ and $^4F_{9/2}$ are not exactly the same.

Several models have been proposed to describe the population of the energy levels of the upconversion "ladder" generated in the *d*, *f*-electrons system.[11,12] As pointed out by Pollnau et al.,[11] the slope decrease is determined by the competition between linear decay (emission processes) and upconversion processes with depletion of the intermediate excited states. Because of high ratio of Yb^{3+}:Er^{3+} in the sample, energy-transfer from Yb^{3+} ions to Er^{3+} ions and excited-stated absorption (ESA) of Er^{3+} ions are the two major mechanisms of upconversion. In order to elucidate the primary characteristics of the upconversion fluorescence, we first adopt a simpler theory by considering only the two photon process for the green and red emission and separate out the main aspects of the mechanism to a specific result by treating some secondary effects as modifications to the main results. Thus, our model is a simple three energy-level system as depicted in Figure 1a.

We take the ground-state population density for both sensitizer (Yb^{3+}) and acceptor (Er^{3+}) ions as N_{0s} and N_0, separately, which are both approximately constant at low pumping power. With p denoting the laser intensity and σ denoting the excitation cross-section, the rate equations describing the excitation mechanisms in the system are

$$\mathrm{d}N_1/\mathrm{dt} = p\sigma_0 N_0 + \gamma N_0 p\sigma_{0s} N_{0s} - \gamma N_1 p\sigma_0 N_{0s} - A_1 N_1 - p\sigma_1 N_1 \qquad (1)$$

$$\mathrm{d}N_2/\mathrm{d}t = \gamma N_1 p\sigma_0 N_{0s} + p\sigma_1 N_1 - A_2 N_2 \qquad (2)$$

where γ is the parameter for the energy transfer upconversion (ETU) and A_i is the total relaxation rate from level i to all lower lying states. For Eq. (1), the terms on the right-hand side describe in sequence, from left to right, the ground-state absorption of Er^{3+}, ETU for Er^{3+} from N_0 to N_1 by excited Yb^{3+}, ETU for Er^{3+} from N_1 to N_2 by excited Yb^{3+}, and decay of N_1 and ESA for Er^{3+} from N_1 to N_2. For Eq. (2), the first two terms have the same meaning as they have in Eq. (1) and A_2N_2 is a term for the relaxation of N_2.

Under steady-state excitation, this yields

$$N_1 = p(\sigma_0 N_0 + \gamma N_0 \sigma_{0s} N_{0s})/(\gamma p\sigma_0 N_{0s} + A_1 + p\sigma_1) \qquad (3)$$

$$N_2 = p(\gamma\sigma_0 N_{0s} + \sigma_1)N_1/A_2 \qquad (4)$$

When the pump power is low and satisfies the condition of $A_1 \gg \gamma p\sigma_0 N_{0s} + p\sigma_1$, linear decay is the dominant depletion mechanism for level 1. From Eq. (3), we obtain $N_1 \propto$ p and consequently, $N_2 \propto pN_1 \propto p^2$.

For medium pumping power that satisfies the condition of $A_1 \approx \gamma p\sigma_0 N_{0s} + p\sigma_1$, there is competition for the depletion of level 1. One path is

linear decay to the lower lying states as in the low-power situation, the other one is upconversion to the level 2 via ETU and ESA. Thus, $N_1 \propto p^m$, where $m < 1$ and results in $N_2 \propto pN_1 \propto p^{1+m} < p^2$.

If the pumping power is high so that $A_1 \ll \gamma p\sigma_0 N_{0s} + p\sigma_1$, the decay from level 1 is overwhelmed by the powerful pumping excitation. The situation here is that only a very small number of ions could relax back to the ground state from level 1, otherwise, they would be upconverted to level 2 by ETU and ESA. A rapid balance between N_1 and the ground state could be reached, thus N_1 becomes a constant and $N_2 \propto pN_1 \propto p$.

First of all, at a given pumping power, the intensity difference between the green and red emission is clearly understood by this model analysis. The variation of population is caused by the different branching ratios of transition processes from N_2 to the emitting states, from $^4F_{7/2}$ to $^4F_{9/2}$ for red and $^4S_{3/2}$ for green, and by multiphonon relaxation–induced nonradiative relaxation, as shown in Figure 1b.

From the simple-rate equations, we show that, as the pumping power increases, the intensity of upconversion fluorescence proportional to N_2 will also increase quadratically at low pumping intensity, but the slope will drop from quadratic to linear at high pumping intensity. This prediction agrees well with our experimental result as shown in Figure 4. In the model analysis, both the green and red emission bands are proportional to N_2 and should exhibit the same trend in pumping power. However, as shown in Figure 4, they have different slopes over the same range of high pumping power; 1.55 for the green band and 1.78 for the red band.

In the simple rate equations of Eq. (1) and Eq. (2), several nonlinear coupling mechanisms that provide additional upconversion or relaxation channels are not included. First of all, a third-step upconversion that populates a higher excited state, N_3, should be considered at high pumping intensity. Direct evidence of such a process that involves three laser photons is the observation of the $^2G_{9/2} \rightarrow {}^4I_{13/2}$ transition fluorescence at 17,938 cm^{-1} and the purple luminescence centered approximately at 24,300 cm^{-1} for the $^2G_{9/2} \rightarrow {}^4I_{15/2}$ transition. In this situation, N_2 tends to be balanced and a portion of N_2 ions are upconverted to N_3, thus not all of the N_2 population contribute to the green and red emission. As a result, we expect a decrease in the quadratic behavior in pumping power dependence. Second, as pointed out by Page et al.,[3] the $^4I_{13/2}$ metastable level tends to act like a bottleneck in upconversion fluorescence emission that retains the Er^{3+} excitation and slows down the increase of upconverson when pumping power increases. As shown in Figure 4, this general behavior is observed in the sample we studied. Based on this model analysis, the red emission and green emission should have the same power dependence even if these two additional mechanisms are considered.

To our knowledge, for upconversion luminescence of Er^{3+}, the dynamics of the red fluorescence have not been studied as well as for the green fluorescence. The exact mechanisms for the different behavior in power

dependence are not well understood. The difference of the two slopes indicates that there must be some additional upconversion channels other than two-photon processes from $^4I_{11/2}$ to $^4F_{7/2}$ that populate subsequently the $^4F_{9/2}$ (red) and $^4S_{3/2}$ (green) multiplets via nonradiative phonon relaxation processes and radiative transitions. The bottleneck effect leads to another possible saturation mechanism of upconversion fluorescence at high laser power by reducing N_0.

For $^4I_{13/2} \rightarrow {}^4F_{9/2}$ upconversion fluorescence, there are a couple of possible mechanisms that populate $^4F_{9/2}$ instead of $^4S_{3/2}$. First, as pointed out by Page et al.,[3] at high pump power, with the increasing population of $^4I_{13/2}$ acting like a bottleneck, the intensity of red emission could be increased through the $^4I_{13/2} \rightarrow {}^4F_{9/2}$ excitation. The difficulty of establishing this mechanism is that this process is off resonance in energy by approximately 1500 cm^{-1} and, therefore, requires a Raman type of nonlinear optical process for energy conversation. Second, a cross-relaxation process that involves $^4F_{7/2} \rightarrow {}^4I_{13/2}$ and $^4I_{15/2} \rightarrow {}^4F_{9/2}$ transitions may also populate the emitting state of $^4F_{9/2}$. This process has an energy mismatch of around -1330 cm^{-1}. As shown in Figure 1b, this cross-relaxation bypasses the green emitting state $^4S_{3/2}$ and populates $^4F_{9/2}$. Therefore, an expected consequence is that at higher Er^{3+} concentration and higher laser intensity, the intensity of green fluorescence relatively diminishes whereas the red fluorescence increases. While we have demonstrated the expected pumping power dependence, the expected effect of concentration dependence was reported by Liang et al.[4]

In fact, upconversion fluorescence of lanthanide ions in solids does not necessarily require resonance of the pumping laser energy with specific absorption energies of the ions, a phenomenon known as the avalanche process.[1,13] A three-level model of an avalanche process in cooperation with cross-relaxation was proposed by Joubert et al.[13] to interpret the upconversion fluorescence induced by nonresonant pumping. If we consider the population bottleneck at $^4I_{13/2}$ as the starting point, the avalanche model can be applied in the current situation to explain the lower saturation of red upconversion at high pumping intensities. The only difference is that the cross-relaxation involves a fourth level (the ground state $^4I_{15/2}$) in our case as elucidated in Figure 1b.

Theoretically, nonlinear coupling similar to four-wave mixing[14,15] would couple the two mechanisms and lead to cooperative transitions to populate $^4F_{9/2}$ levels for red luminescence. With regard to energy conservation, such a mixing is favorable. Given that upconversion into the purple region requiring three laser photons has been observed in the sample, an excited-state absorption ($^4I_{13/2} \rightarrow {}^4F_{9/2}$) that coherently couples to a cross-relaxation at high laser intensity is not unrealistic. As demonstrated by Liang et al.,[4] the intensity ratio of the green to red upconversion fluorescence is indeed sensitive to the Er^{3+} concentration, which suggests that Er^{3+} to Er^{3+} energy transfer plays an important role. Although further investigations are needed to evaluate the contribution and make comparisons with experimental results, these cooperative transitions provide a qualitative explanation why the

slope of the red emission decreases more slowly than the green emission with increasing of laser intensity.

CONCLUSIONS

Because of the high efficiency of upconversion fluorescence, powdered crystals of hexagonal sodium yttrium fluoride, $NaYF_4$, doped with Er^{3+} and Yb^{3+} have been studied in an attempt at understanding the pump-power dependence of the green and red fluorescence bands. For the regular downconversion cascade relaxation after UV excitation, the green and red fluorescence bands have approximately the same intensity. However, in upconversion, the red band is much weaker than the green band because of restricted relaxation channels for populating the red emitting state of $^4F_{9/2}$. The ratio of green and red fluorescence intensities is different between UV excitation and IR excitation. The intensity of both green and red upconversion fluorescence bands is affected at high pumping intensities by a low-lying state acting like a bottleneck. We have shown that the green band and red band have different pumping power dependencies. The effect on upconversion is less significant for the red fluorescence than for the green. This phenomenon is attributed to cross-relaxation and a secondary upconversion processes that only populates the $^4F_{9/2}$ levels. Known as the avalanche process, this effect occurs with pump energies increasing above a threshold. Given the potential applications of this efficient upconversion phosphor, a clear understanding of the upconversion dynamics is important in providing guidance in materials development and application.

ACKNOWLEDGMENT

Work at Argonne National Laboratory was performed under the auspices of the U.S. Department of Energy, Office of Basic Energy Sciences, Division of Chemical Sciences, Geosciences and Biosciences, under contract no. W-31-109-ENG-38.

REFERENCES

1. Auzel, A. Up-conversion in RE-doped solids. In *Spectroscopic Properties of Rare Earths in Optical Materials*; Liu, G. K. and Jacqiuer, B., (eds); Springer and TUP: Berlin, 2005; Chapter 5, 266–319.
2. Johnson, L. F.; Guggenheim, H. J.; Rich, T. C.; Ostermayer, F. W. Infrared-to-visible conversion by rare-earth ions in crystals. *J. Appl. Phys.* **1972**, *43*, 1125–1137.
3. Page, R. H.; Schaffers, K. I.; Waide, P. A.; Tassano, J. B.; Payne, S. A.; Krupke, W. F.; Bischel, W. K. Upconversion-pumped luminescence efficiency

of rare-earth-doped hosts sensitized with trivalent ytterbium. *J. Opt. Soc. Am. B* **1998**, *15*, 996–1008.
4. Liang, L.; Wu, H.; Hu, H.; Wu, M.; Su, Q. Enhanced blue and green upconversion in hydrothermally synthesized hexagonal $NaY_{1-x}Yb_xF_4:Ln^{3+}$ ($Ln^{3+} = Er^{3+}$ or Tm^{3+}). *J. Alloy. Compd.* **2004**, *368*, 94–100.
5. Krämer, K. W.; Biner, D.; Frei, G.; Güdel, H. U.; Hehlen, M. P.; Lüthi, S. R. Hexagonal sodium yttrium fluoride based green and blue emitting upconversion phosphors. *Chem. Mater.* **2004**, *16*, 1244–1251.
6. Yi, G.; Lu, H.; Zhao, S.; Ge, Y.; Yang, W.; Chen, D.; Guo, L. H. Synthesis, characterization, and biological application of size-controlled nanocrystalline $NaYF_4$:Yb,Er infrared-to-visible up-conversion phosphors. *Nano. Lett.* **2004**, *4*, 2191–2196.
7. Luo, L.; Zhang, X. X.; Li, K. F.; Cheah, K. W.; Shi, J. X.; Wong, W. K.; Gong, M. L. Er/Yb doped porous silicon—a novel white light source. *Adv. Mater.* **2004**, *16*, 1664–1667.
8. Heer, S.; Kömpe, K.; Güdel, H. U.; Haase, M. Highly efficient multicolour upconversion emission in transparent colloids of lanthanide-doped $NaYF_4$ nanocrystals. *Adv. Mater.* **2004**, *16*, 2102–2105.
9. Kano, T.; Yamamoto, H.; Otomo, Y. $NaLnF_4:Yb^{3+},Er^{3+}$ (Ln:Y,Gd,La): efficient green-emitting infrared-excited phosphors. *J. Electrochem. Soc.* **1972**, *119*, 1561–1521.
10. Menyuk, N.; Dwight, K.; Pierce, J. W. $NaYF_4$:Yb,Er—an efficient upconversion phosphor. *Appl. Phys. Lett.* **1972**, *21*, 159–161.
11. Pollnau, M.; Gamelin, D. R.; Lüthi, S. R.; Gsgdel, H. U. Power dependence of upconversion luminescence in lanthanide and transition-metal-ion systems. *Phys. Rev. B* **2000**, *61*, 3337–3346.
12. Suyver, J. F.; Aebischer, A.; García-Revilla, S.; Gerner, P.; Güdel, H. U. Anomalous power dependence of sensitized upconversion luminescence. *Phys. Rev. B* **2005**, *71*, 1–91251231.
13. Joubert, M. F.; Guy, S.; Jacquier, B. Model of the photon-avalanche effect. *Phys. Rev. B* **1993**, *48*, 110031–10037.
14. Yariv, A.; Pepper, D. M. Amplified reflection, phase conjugation, and oscillation in degenerate four-wave mixing. *Opt. Lett.* **1977**, *1*, 16–18.
15. Schmitt-Rink, S.; Varma, C. M.; Levi, A. F. Excitation mechanisms and optical properties of rare-earth ions in semiconductors. *J. Phys. Rev. Lett.* **1991**, *66*, 2782–2785.